Chemical Characterization of Titan's Tholins: Solubility, Morphology and Molecular Structure Revisited†

N. Carrasco,*,‡ I. Schmitz-Afonso,§ J-Y. Bonnet,|| E. Quirico,|| R. Thissen,|| Odile Dutuit,|| A. Bagag,§ O. Laprévote,§ A. Buch,⊥ A. Giulani,#,▽ Gilles Adandé,|| F. Ouni,‡ E. Hadamcik,‡ C. Szopa,‡ and G. Cernogora‡

Université de Versailles St-Quentin, UPMC Univ. Paris 06 CNRS/INSU, LATMOS-IPSL, Route des Gâtines, 91371 Verrières le Buisson Cedex, France, Institut de Chimie des Substances Naturelles, CNRS, Bât. 27, Avenue de la Terrasse 91198 Gif-sur-Yvette Cedex, France, Laboratoire de Planétologie de Grenoble, CNRS, UJF, UMR 5109, BP 53, 38041 Grenoble Cedex 9, France, Laboratoire de Génie des Procédés et Matériaux, Ecole Centrale Paris, Grande Voie des Vignes - 92295 Chatenay-Malabry Cedex, France, SOLEIL, L'Orme des merisiers, Saint Aubin BP48, 91192 Gif sur Yvette Cedex, France, and Cepia, Institut National de la Recherche Agronomique (INRA), BP 71627, F-44316 Nantes Cedex 3 France

Received: May 20, 2009; Revised Manuscript Received: August 25, 2009

In this work Titan's atmospheric chemistry is simulated using a capacitively coupled plasma radio frequency discharge in a N_2-CH_4 stationnary flux. Samples of Titan's tholins are produced in gaseous mixtures containing either 2 or 10% methane before the plasma discharge, covering the methane concentration range measured in Titan's atmosphere. We study their solubility and associated morphology, their infrared spectroscopy signature and the mass distribution of the soluble fraction by mass spectrometry. An important result is to highlight that the previous Titan's tholin solubility studies are inappropriate to fully characterize such a heterogeneous organic matter and we develop a new protocol to evaluate quantitatively tholins solubility. We find that tholins contain up to 35% in mass of molecules soluble in methanol, attached to a hardly insoluble fraction. Methanol is then chosen as a discriminating solvent to characterize the differences between soluble and insoluble species constituting the bulk tholins. No significant morphological change of shape or surface feature is derived from scanning electron microscopy after the extraction of the soluble fraction. This observation suggests a solid structure despite an important porosity of the grains. Infrared spectroscopy is recorded for both fractions. The IR spectra of the bulk, soluble, and insoluble tholins fractions are found to be very similar and reveal identical chemical signatures of nitrogen bearing functions and aliphatic groups. This result confirms that the chemical information collected when analyzing only the soluble fraction provides a valuable insight representative of the bulk material. The soluble fraction is ionized with an atmospheric pressure photoionization source and analyzed by a hybrid mass spectrometer. The congested mass spectra with one peak at every mass unit between 50 and 800 u confirm that the soluble fraction contains a complex mixture of organic molecules. The broad distribution, however, exhibits a regular pattern of mass clusters. Tandem collision induced dissociation analysis is performed in the negative ion mode to retrieve structural information. It reveals that (i) the molecules are ended by methyl, amine and cyanide groups, (ii) a 27 u neutral moiety (most probably HCN) is often released in the fragmentation of tholin anions, and (iii) an ubiquitous ionic fragment at *m*/*z* 66 is found in all tandem spectra. A tentative structure is proposed for this negative ion.

1. Introduction

Titan, the largest satellite of Saturn, has a dense atmosphere composed of nitrogen (95 to 98%), methane, molecular hydrogen, and traces of hydrocarbons. Several nitrogen-bearing organic compounds such as hydrogen cyanide (HCN), cyanoacetylene (HC_3N), and cyanogen (C_2N_2) have been detected in its atmosphere.[1,2]

A further chemical growth, initiated by the activation of N_2 and CH_4 is at work, leading to strong interest and relevance for astrobiological questions. The atmospheric chemistry is so active that it eventually produces macroscopic particles that sediment slowly in the atmosphere, leading to the brownish haze permanently surrounding the satellite. These organic aerosols play an important role in the properties and evolution of Titan's atmosphere.[3] Indeed, aerosols absorb a significant fraction of the incoming sunlight, generating an antigreenhouse effect that cools down Titan's surface.[4] However, information on these aerosols composition, their formation, and their growth is still very limited due to the difficulty to perform observations of Titan's upper atmosphere from the Earth or from space probes.[5]

A complementary strategy to remote observations was developed. The study of Titan's aerosols was refined by producing analogous materials in laboratory, the so-called Titan tholins. The most efficient production methods are plasma discharges in gaseous N_2-CH_4 mixtures.[6−13] In the present work, the discharge is based on a radio frequency capacitively coupled plasma.[14]

† Part of the special section "Chemistry: Titan Atmosphere".
* Corresponding author. E-mail: nathalie.carrasco@latmos.ipsl.fr.
‡ Université de Versailles St-Quentin.
§ Institut de Chimie des Substances Naturelles CNRS.
|| Laboratoire de Planétologie de Grenoble, CNRS.
⊥ Ecole Centrale Paris.
SOLEIL.
▽ Institut National de la Recherche Agronomique.

10.1021/jp904735q CCC: $40.75
Published on Web 09/23/2009

In this work two different tholin samples have been generated by changing the relative abundance of N_2/CH_4 inlets in the plasma; either 98/2% (SA98) or 90/10% (SA90). They are similar to previous tholin production conditions[8,14−16] and representative of the methane molar fraction profile measured[17] in Titan's atmosphere.

The aim is very different from previous solubility studies[8,15,16] that were focused on a possible extrapolation of Titan's aerosols' solubilities with putative liquid interfaces on Titan's surface/subsurfaces or in atmospheric droplets. In this study, the aim is to know whether the laboratory analyses made on the easily accessible soluble fractions are representative or not of the bulk tholins. The choice of the solvent is thus decorrelated from any considerations about the actual solvatation processes on Titan's surface. It ensures that the tholins organic matter is significantly partitioned into two phases (soluble or insoluble fractions) to further investigate the morphology and chemical nature of both the solid and dissolved compounds through complementary analyses. To further characterize both soluble and insoluble phases, we first developed a new protocol to evaluate quantitatively the solubility of the samples and we measured the solubility of samples SA98 and SA90 in one polar (methanol) and in one nonpolar (toluene) solvent.

The fractions were further subjected to the following analytical methods:

• Scanning electron microscopy (SEM) was used to evaluate the effect of solubilization on the morphology of the samples.

• Infrared (IR) absorption spectroscopy was used to evaluate the potential chemical partitioning occurring in the SA90 and the SA98 samples when the soluble fraction was separated from the insoluble one.

• Atmospheric pressure photoionization (APPI) coupled with a hybrid quadrupole time-of-flight mass spectrometry (QTOF-MS) was used to evaluate the molecular composition of the soluble fraction of both samples. Further analysis by the tandem collision induced dissociation (CID) method led to structural information concerning the negatively charged ionic species present in the spectrum.

2. Experimental Methods

2.1. PAMPRE Experimental Setup and Tholins Production and Collection. The experimental set up named PAMPRE (French acronym for Production d'Aérosols en Microgravité par Plasma REactifs) was described in detail previously[14] and is summarized here briefly. The plasma is a radio frequency capacitively coupled plasma discharge produced at a 13.56 MHz frequency in a N_2-CH_4 gaseous mixture. The plasma is confined in a cylindrical cage shaped by a metallic grid of 138 mm in diameter and 45 mm length. In the plasma discharge, electrons dissociate and ionize N_2 and CH_4. This initiates chemical reactions and molecular growth producing hydrocarbons and nitrogen bearing molecules that eventually end up forming solid particles. The produced solid particles are negatively charged and maintained in levitation between the electrodes by electrostatic forces. The charge increases with tholin size. The N_2-CH_4 gaseous mixture is injected continuously into the plasma reactor, as a neutral flow oriented downward. This produces a neutral drag force, which can eject the solid particles out of the plasma discharge. The ejected tholins are trapped in a glass vessel surrounding the metallic cage. When sufficient amounts of tholins are produced (i.e., usually 8 h), the plasma is turned off; the reactor is thoroughly pumped to evacuate potential traces of HCN and other residual gases, then filled with N_2 to atmospheric pressure and opened for solid sample collection. Under usual conditions, about 0.5 cm^3 (∼100 mg) of solid material is produced in a run of 8 h. The tholins, which have the appearance of a very fine orange to brown powder, are deposited gently in the glass vessel without any interaction with the substrate. They are collected into microvials for ex-situ analyses.

In this work, the samples were obtained in the following operating conditions: a total pressure of 1 mbar, a flow rate of 55.0 ± 0.1 sccm, and an absorbed radio frequency power of 30 ± 2 W. Two different samples were produced by adjusting the relative flux of N_2 vs CH_4. The first sample (SA98) was produced with a gaseous mixture containing $2.00 \pm 0.06\%$ of methane, while the second sample (SA90) was produced with a mixture containing $10.0 \pm 0.2\%$ of methane. Experiments were performed at room temperature, which is not representative of Titan's atmosphere low temperature (100−200 K). The influence of temperature on kinetics and mechanisms is beyond this work but is a major concern for further studies on Titan's tholins.

2.2. Scanning Electron Microscopy. The morphology and size of the particles of both samples were investigated by field emission gun scanning electron microscopy (FEG-SEM). Aerosols were deposited on an aluminum plate and coated with a thin layer (20 nm) of gold to make their surface electrically conducting. Then, observations were achieved with an FEG-SEM (JEOL) equipped with an X-ray detector.[18]

2.3. Infrared Spectroscopy Analysis. Measurements by infrared spectroscopy were performed on the soluble and insoluble fractions of SA90 and SA98 samples, as well as on acid treated SA90. The sample for soluble fraction spectroscopy was produced as follows. The fine powder (a few milligrams) collected from the PAMPRE setup was put into a polypropylene microtube. Then 1 mL of methanol per mg of tholins was added, and the sample was sonicated for 30 min and centrifugated for 15 min at 800*g*. The slightly colored soluble fraction was then collected and deposited onto a BaF_2 window, by repeated sequences of droplets deposition and methanol evaporation. The pure sample, as well as the dried powder containing the insoluble fraction were also deposited and crushed between two BaF_2 windows. The final thin film samples were dried at ambient temperature under a low pressure of about 550 mbar for at least 2 h to evaporate the remnant methanol from the samples (soluble and insoluble). Measurements were performed with a micro-FTIR infrared microscope HYPERION3000 (Bruker Inc.) in the spectral range 4000−700 cm^{-1} with 4 cm^{-1} spectral resolution.

2.4. Mass Spectrometry: APPI. In this set of experiments, the samples were ionized by the atmospheric pressure photoionization (APPI) technique and analyzed by a hybrid quadrupole-time-of-flight mass spectrometer (Q-star pulsar *i* from Applied Biosystems) with a resolution of 0.15 u in the full mass range (from 50 to 1000 u). The photoionization of soluble fractions took place in the Photospray source (Applied Biosystems) fitted with a Krypton PKS 106 lamp that generates mainly 10.6 eV photons.

The extraction procedure was carried out on both SA98 and SA90 samples. First, 10 mg of tholins was dissolved in 10 mL of solvent (methanol or toluene). Each sample was stirred vigorously with a vortex for 1 h at room temperature and then filtered through a 0.2 μm Teflon membrane.

The extracted samples were injected into the mass spectrometer by the flow-injection analysis (FIA) method: 20 μL of solutions was loaded into an injection loop and next eluted with the base solvent at a flow rate of 200 μL min^{-1} for methanol and 150 μL min^{-1} for toluene. Toluene was used as dopant at 15 μL min^{-1} in methanol extracts. Operating

TABLE 1: Tholins Solubility (mg mL^{-1}) Obtained after Partial Dissolution of a Known Amount of Tholins in a Given Amount of Solvent[a]

	Coll et al.[8]	Sarker et al.[16]	this work	McKay[15]
operating conditions	2% CH_{42}	2%	2%	10% CH_4, 1150 mb
C/N ratio	2.8	1.8	2.3	5.5
solubility in	ND			
water		4.4	0.20	0.5
methanol	ND	ND	0.30	0.5
acetonitrile	4	ND	0.43	ND

[a] For each sample, the ratio of C/N retrieved from elementary analysis is indicated. ND: no data available.

parameters were heating temperature = 400 °C, ion source voltage = +1500 V or −1200 V, declustering potential = +10 V or −10 V, focusing potential = +40 V or −50 V (positive or negative potentials were adjusted to produce optimum flux of either positively or negatively charged ions, respectively). Tandem mass spectrometry experiments in negative ion mode were carried out with nitrogen as collision gas and collision energy at −20 or −35 V.

3. Results and Discussions

3.1. Solubility Properties of Tholins in Both Polar and Nonpolar Solvents. ***Comparison with the Protocol Previously Used in Tholins Solubility Studies.*** To compare the solubility properties of PAMPRE tholins with the already published literature, we first followed the protocol described in McKay,[15] which can be summarized into four steps: (i) mixing of a known quantity of tholins into a known amount of solvent; (ii) filtration of the cloudy solution; (iii) evaporation of the solvent; (iv) measurement of the mass of the remaining solid material. This method is the standard method to measure the solubility for a pure material as it usually refers to the concentration of the substance in a liquid that has reached equilibrium with the substance in solid phase (e.g., adding more solid no longer increases the concentration in the liquid phase, it just increases the solid's phase volume).

To do so, we measured with 10^{-2} mg precision, a well-defined amount of SA98 tholins (about 10 mg) and added 10 mL of solvent (methanol or toluene). The solution was then stirred vigorously with a vortex for 1 h at room temperature. The resulting cloudy mixture was filtered through a calibrated 0.2 μm Teflon membrane, known to be able to retain all solid material.[14] To measure the partitioning between insoluble fraction and soluble fraction, the solvent was removed from both fractions using a vacuum rotavapor. This operation was done at 30 °C to avoid tholin thermal degradation. The solid dry material was then weighted.

Table 1 presents a summary of the results and their comparison with those of McKay et al.,[15] Coll et al.,[8] and Sarker et al.[16] The conditions of tholin production in these studies are summarized in Table 2. In all these studies, solubility was supposedly achieved by a partial dissolution of the tholins samples in a given solvent.

The solubility found by McKay et al. has to be considered separately because in that case tholins were produced under very specific conditions: 10% of methane, and at a pressure slightly above atmospheric pressure. Their samples hence are specific because they contain much more carbon (C/N = 5.5) than the tholins analyzed in the other studies.

A surprising result is the low solubility in polar solvents of the PAMPRE tholins in comparison with the tholins produced by Coll et al.[8] and by Sarker et al.[16] (about 10 times less soluble). Indeed, the samples were produced almost in the same operating conditions (see Table 2): low pressure, about 2% CH_4 in the gaseous mixture and a gas residence time of a fraction of second. Moreover, the elemental compositions of the three tholins are quite similar: C/N = 2.3 for the PAMPRE samples, C/N = 2.8 for the tholins of Coll et al., C/N = 1.8 for the tholins of Sarker et al., suggesting the development of a similar chemistry within the plasma. This result allows us to realize that the so-called "solubility" used in the previous studies may not be a good indicator of the solubility properties for tholins. Indeed, these are nonhomogeneous solids, containing a huge amount of different compounds (as to be shown below by the APPI-TOF analysis, and as was shown by Sarker et al.[16]). Each one has its own solubility and according to the broad mass distribution observed by APPI-TOF analysis, a number of molecules may be still completely soluble in the used volume of solvent, whereas larger molecules may be at the saturation equilibrium since the very first microliter of solvent.

TABLE 2: Comparison of Plasma Reactors Operating Conditions for Tholins Production

experimental device	PAMPRE (this work)	Coll et al.[8]	Sarker et al.[16]
frequency	13.6 MHz	DC	60 Hz (mains)
length of the plasma path (mm)	45	250 + 250	450
diameter (mm)	138	18 and 9	supposed 10 or 18
pressure (mbar)	1	2	10
gas flow (sccm)	55	83	100
temperature (K)	ambiant	≈100−150	195
CH_4/N_2 (%)	2 and 10	2	0.5 to 8
gas residence time into the plasma (s)	≈0.7	≈0.3	≈0.3 or 1

Tholins can be compared with polymers.[19] The solubility of polymers and its measurement have been described by the Flory−Huggins theory in the early 40s.[20−23] This approach has also been followed by Raulin[24] for Titan. Three different cases are reported: (i) the polymer and solvent are totally immiscible over the entire composition range and will coexist as two distinct phases; (ii) the polymer and solvent are totally miscible, (iii) the polymer and solvent are partially miscible and a solution that contains such a polymer will separate into two phases containing different compositions of both components. In this case, phase equilibrium is hardly guaranteed, and quantitative evaluation is difficult. In the case of tholins, we are facing the third type of situation.

To confirm this hypothesis for our samples, we checked that a higher "solubility" could be obtained with the same tholins by adding systematically a supplementary amount of solid in a supposedly saturated solution (coexistence of solid and solution), showing that no stable value of solubility was reached with such a protocol for tholins.

We therefore extended the previous protocol to approach a satisfactory quantity to describe the solubility of the PAMPRE tholins. This was done in one polar and one nonpolar solvent.

Solubility Ratio and Average Solubility of the Soluble Part of PAMPRE Tholins. We propose that a better criterion to characterize and intercompare the solubility of the samples is (i) first to quantify the solubility ratio of the samples, i.e., the ratio between insoluble nucleus and soluble molecules, and (ii) quantify an average solubility of the soluble part itself, i.e., the maximum equilibrium concentration for the soluble material. The results are reported in Table 3 and illustrated in the case of SA90 in methanol in Figure 1.

(i) Solubility Ratio. Increasing concentrations of raw tholins in methanol were tested (up to 8 mg mL^{-1}) according to the

TABLE 3: PAMPRE Tholins Solubility Ratio and Average Solubility of the Soluble Fraction in Methanol and Toluene[a]

	solubility ratio (%)		average solubility (mg mL^{-1})	
solvent	SA98	SA90	SA98	SA90
methanol	19 ± 6	35 ± 5	2.5 ± 0.2	6.2 ± 0.6
toluene	3	5	ND	ND

[a] In the case of methanol extraction, measurements were repeated three or four times for solubility ratio determinations and twice for average-solubility determinations (reported uncertainty corresponds to the standard deviation). In the case of the toluene extraction, the low solubility of the samples and the viscosity of the solvent led to a difficult separation between the soluble and the insoluble fractions. The uncertainty on this determination is large for toluene and the protocol was not repeated more than once in this case.

protocol described above. Both insoluble and soluble fractions were retrieved. This allowed quantifying a mass ratio between the soluble mass and the total mass of the original sample.

A large mass ratio was found in methanol: 19 and 35% for SA98 and SA90, respectively, whereas the soluble fraction in toluene is only on the order of 3−5% of the total mass for both samples SA98 and SA90. The latter is hence close to the uncertainty on the values. This confirms the trend noticed by Coll et al. and McKay et al.[8,15] concerning the large affinity of tholins with polar solvents and a much lower one with nonpolar solvents. Following this, and according to the rule of thumb that "like dissolves like", tholins have a large content of polar molecules and, the fraction of nonpolar molecules is probably very limited, if it exists at all.

(ii) Average Solubility of the Soluble Fraction. A second step allowed us to determine the average solubility at saturation of the solution in methanol ("average" again because there is no guarantee that the soluble fraction is homogeneous; the so-called solubility refers here to the total concentration of all soluble compounds included in the tholins and not the concentration of a pure compound). The dried soluble fraction was partially dissolved in a limited amount of solvent to observe the coexistence of both a precipitate and a colored solution. The resulting mixture was filtered and the soluble part was then evaporated and weighted. Solubility at saturation was thus determined at 6.2 mg mL^{-1} for the SA90 sample and at 2.5 mg mL^{-1} for the SA98 sample.

Even in a polar solvent like methanol, most of the organic matter remains insoluble (65% for SA90 and 81% for SA98). The reason for such an amount of nonsoluble fraction within PAMPRE tholins comes likely from the growth process occurring in the plasma discharge. It seems that plasma processes using levitation allow the production of species containing long molecules, which are no longer soluble in any solvent. Hence tholins produced in PAMPRE consist in a limited fraction of polar molecules readily removable attached to a large and insoluble nucleus.

3.2. Analysis of the Remaining Insoluble Fraction by SEM (Scanning Electron Microscopy). The analysis by SEM of the integer samples SA98 and SA90 has been described in Hadamcik et al.,[18] showing a distribution of globally spherical grains, more or less regular, isolated or coalescent. In the same plasma conditions as the ones used for tholins production in the present work, a mean grain diameter of 315 ± 185 nm with diameters reaching 1400 nm for the largest detected grains has been measured for the SA98 sample, and a mean grain diameter of 595 ± 390 nm with diameters reaching 2500 nm for the largest detected grains for the SA90 sample (the uncertainty reported here is the half-maximum width of the Gaussian size grain distributions). More than one thousand grain diameters are measured on SEM images to obtain a good statistic of the size distributions. Each grain seems to be an aggregate with an apparent radial structure. The SA90 sample grains seem to be more porous than the grains of SA98.

After extraction and recovery of the insoluble fraction, as described in the previous section, a new snapshot of the samples was taken by SEM. The shape of the tholins is not modified by the previous liquid extraction and the sample shows again a Gaussian size distribution of spherical grains. Figure 2 shows some examples of the bulk tholins and their insoluble part. The surface appearance of the grains seems to be protected from the extraction process. The characteristic cauliflower feature of SA98 surface is, for example, also observable on the insoluble remaining grains. The average diameter of the grains is possibly reduced in comparison with the bulk sample: 290 nm instead of 315 nm for SA98 and 450 nm instead of 595 nm for SA90. This decrease is compatible with the mass loss of SA98 but is more important for SA90. After extraction, the SA90 sample seems to present more debris due possibly to the long mechanical stirring of grains which are on average bigger and maybe more fragile in SA90 than in SA98. The important size decrease of the insoluble part of SA90 may thus be explained by the contribution of these small fragments. The hypothesis of superficial smaller molecules is quite probable but needs to be confirmed by improving the precision on the average diameter of the particles.

The preservation of the tholins global structure despite the application of an efficient extraction stress (35% of the organic matter has been pulled out in methanol for sample SA90 for example) is in favor of a solid structure despite its important porosity.

The high porosity of the grains is confirmed by a solvent accessibility experiment, based on an acidic hydrolysis of the SA98 sample. The SA98 powder was exposed for 1 week at room temperature to a 12 mol L^{-1} HCl liquid solution. This exposition led to the attack of the terminating −CN functional groups. IR measurements revealed that this group fully disappeared in the spectra and therefore that any part of the tholins, soluble or insoluble, could be reached by the solvent (see Figure 3). On every IR spectra, the structure appearing between 2300 and 2400 cm^{-1} is the signature of atmospheric CO_2.

3.3. Comparison of Soluble and Insoluble Fractions in Methanol by IR Spectroscopy. The spectra of soluble, insoluble, and raw samples of SA90 and SA98 are displayed in Figure 4. The spectra are divided into four regions of

TABLE 4: Main Ionic Fragments and Neutral Mass Loss Observed for a Few Main Species by Collision Induced Dissociation Tandem Analysis of Negatively Charged Ions from Tholins Soluble Fraction in Methanol

	precursor (*m*/*z*)	collision energy (eV)	fragments (*m*/*z*)											neutral mass loss (u)
SA98	93	−20	65	66										28, 27
	117	−35	65	66			90							52, 51, 27
	141	−35	65	66	88	89	90				114			76, 75, 53, 52, 51, 27
SA90	117	−35	65	66										52, 51
	134	−35	65	66				92	107	119				69, 68, 42, 27, 15
	149	−35	65	66					107			122	134	84, 85, 42, 27, 15

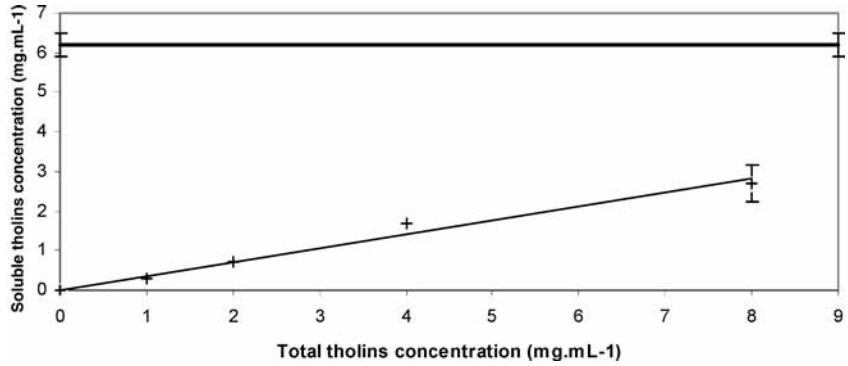

Figure 1. Determination of the soluble fraction and the average solubility of the soluble ratio for sample SA90 in methanol. The soluble ratio corresponds to the slope of the straight line. The average solubility (horizontal line) is obtained after evaporation of the solvent from the isolated soluble fraction; and resolubilization of the soluble sample in a minimum of solvent.

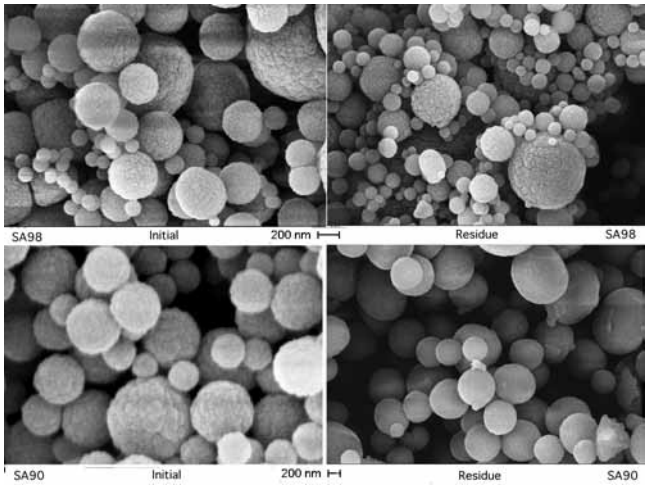

Figure 2. Electronic microscopy observations of tholins before (left) and after (right) extraction in methanol (top, SA98; bottom, SA90).

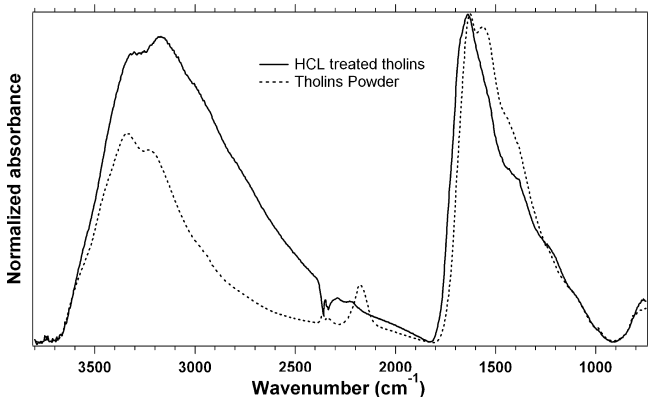

Figure 3. IR spectra of SA98 tholins before and after an HCl acid attack.

interest: region I (3000−3700 cm^{-1}), region II (2700−3000 cm^{-1}), region III (2000−2300 cm^{-1}), and region IV (900−1800 cm^{-1}).

The results are similar for SA98 and SA90. The three infrared spectra (bulk/insoluble/soluble fractions) exhibit only slight differences. Region I contains spectral features due to the symmetric and antisymmetric vibrational stretching modes of primary, and possibly secondary, amine functional groups.[25] The ratio of peak intensities of these bands is different between soluble and insoluble fractions. In region II, the intensities of the alkyl bands, with peaks at ∼2920 and ∼2960 cm^{-1} (symmetric and antisymmetric stretching modes of C−H in CH_2 and CH_3), are higher in the soluble fraction than in the insoluble one. This statement is confirmed by the more intense symmetric and antisymmetric bending modes of $-CH_2$ and $-CH_3$ peaking at 1380 and 1460 cm^{-1}, respectively (region IV). This suggests a higher content of aliphatic chains in the soluble fraction.

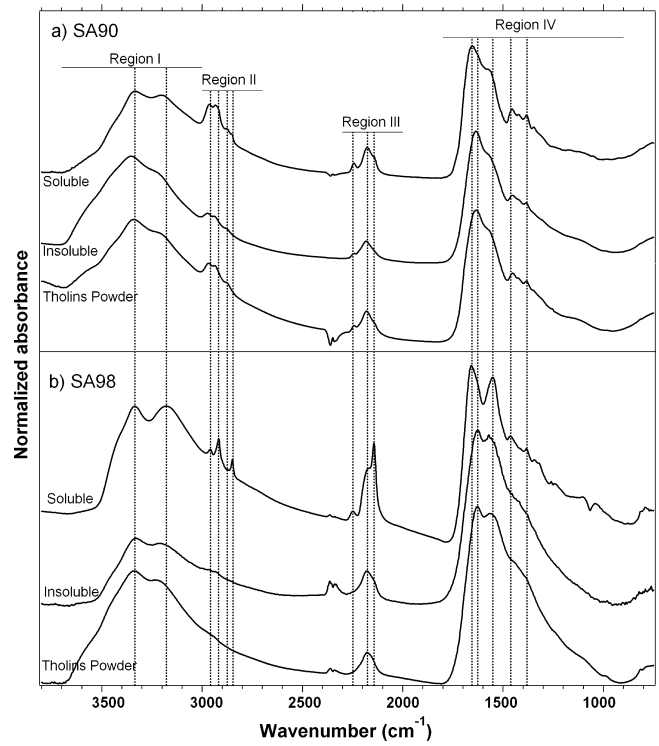

Figure 4. IR spectra of (a) the SA90 tholin and its soluble and insoluble fractions and (b) the SA98 tholin and its soluble and insoluble fractions. Band assignments are given in the text.

The broad and complex pattern at ∼2200 cm^{-1} also exhibits a slight evolution, as the weak band at 2240 cm^{-1} is more intense and better separated from the rest of the pattern in the soluble than in the insoluble fraction. This band can be confidently assigned to a cyanide functional group −CN (branched on an aliphatic group), whereas the broad structured pattern can be assigned to either conjugated nitriles and/or isocyanide. As unsaturation decreases with aliphaticity, these results would favor the former interpretation that there are fewer conjugated cyanides in the soluble fraction.

The spectral region IV exhibits spectral congestion. The broad band peaking at 1630 cm^{-1} in both the raw tholins powder and the insoluble fraction, is displaced at 1650 cm^{-1} in the spectrum of the soluble fraction. The other intense band peaks at ∼1560

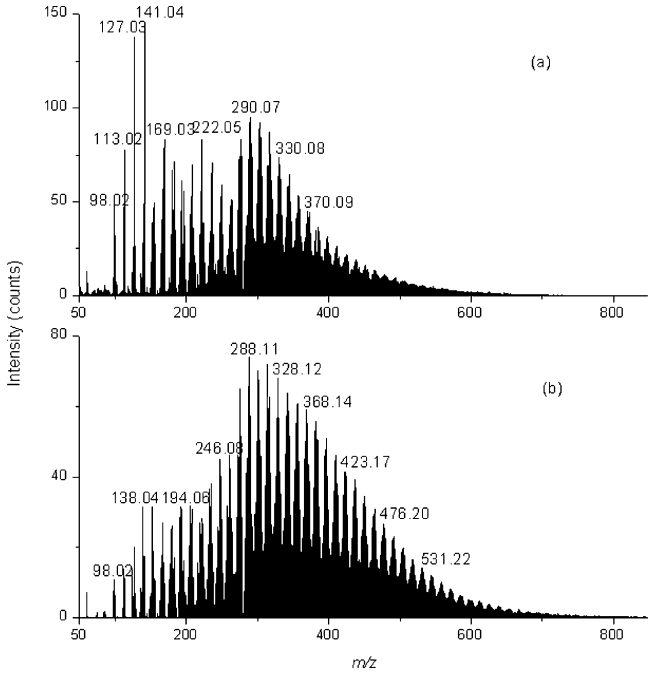

Figure 5. APPI mass spectra of tholins soluble fraction in methanol in positive ion mode: (a) SA98; (b) SA90. CH_4 inlet percentage effect on tholins composition.

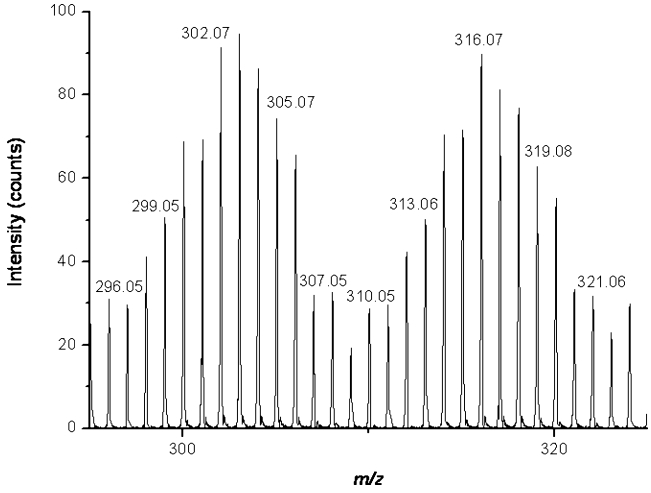

Figure 6. Enlargement of the APPI mass spectrum of sample SA98 between *m/z* 295 and 325.

cm^{-1} and shows no particular evolution in all the spectra. These bands involve the contribution of C═N groups, as imine and/or in N-bearing heteroaromatic or heterocyclic groups. Previous studies[16,26] showed that unsaturations were most probably located on nitrogen. No C═C bonds are thus expected in the IR spectra. However, the contribution of the scissors deformation of the $-NH_2$ amine group is expected to range between around 1650 and 1550 cm^{-1},[27] precluding a clear assignment of this spectral region.

To summarize this section, the infrared spectra of insoluble and soluble fractions of SA90 are very similar; the soluble fraction contains most, probably all, the functional groups that form the insoluble fraction. Hence, a study by mass spectrometry of the sole soluble fraction provides a valuable insight representative of all tholins.

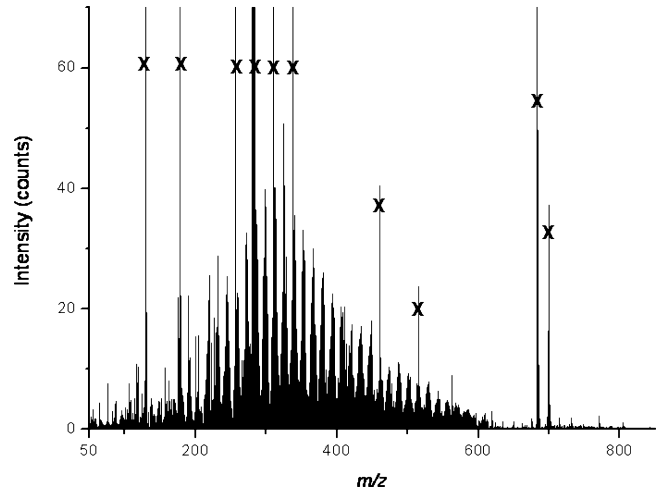

Figure 7. APPI mass spectrum of SA90 tholins soluble fraction in toluene in positive ion mode. Peaks labeled by and X are impurities also found in the blanks.

4. Analysis of the Soluble Fraction by Mass Spectrometry Analysis

4.1. Ionization Methods. The choice of the ionization method has been dictated by the aim to compare by mass spectrometry the molecular content of the soluble fractions resulting from solubilization in either methanol or toluene using the same ion source. While electrospray ionization (ESI) is not producing usable signals with nonpolar solvents such as toluene, atmospheric pressure photoionization (APPI) is.[28] APPI is a relatively recent method.[29] The technique is based on the irradiation of a heated atmospheric spray containing the solvent and the analyte molecules by EUV photons of known energy. Usually, when the solvent has an ionization potential higher than the photon energy, an additional solvent, referred to as the dopant in the following, is introduced concomitantly in the source. Direct photoionization of the solvent or photoionization of the dopant generates reactive ionic species, which can eventually ionize the analyte molecules. In the positive ion mode, this chemical ionization produces protonated molecules and radical cations upon proton transfer and charge transfer, respectively. In the negative ion mode, deprotonated molecules and radical anions can form by proton transfer, electron transfer, or electron attachment. This whole range of ionization mechanism is a further guarantee of the universal integral character of this ionization method, as it is able to reveal almost any type of analyte in the solution, independently of their chemical functionality. In this work, toluene extracts did not require any dopant, because the ionization potential of toluene is lower than the 10.6 eV photons of the lamp. For methanol extracts, there is the need to use a dopant. To allow proper comparison of the mass spectra recorded in toluene, the latter was used as a dopant.

4.2. Mass Spectra in Positive Ion Mode. Considering the solubility results, soluble fractions of both samples (SA98 and SA90) in methanol and in toluene were analyzed using APPI in the positive ionization mode.

For both SA98 and SA90 in methanol, the mass spectra show a complex spectrum (see Figure 5) containing a very large distribution of ions from $m/z = 50$ to m/z 800 (i.e., the full analysis range of the instrument), organized in regularly spaced clusters separated by 13 or 14 u. As can be seen in the spectra, the intensity of the observed features are quite different; increasing the CH_4 mixing ratio (SA90) favors the presence in the spectrum of heavier species. The spectra show peaks at every mass unit between *m/z* 100 and 800 (see a zoom between *m/z*

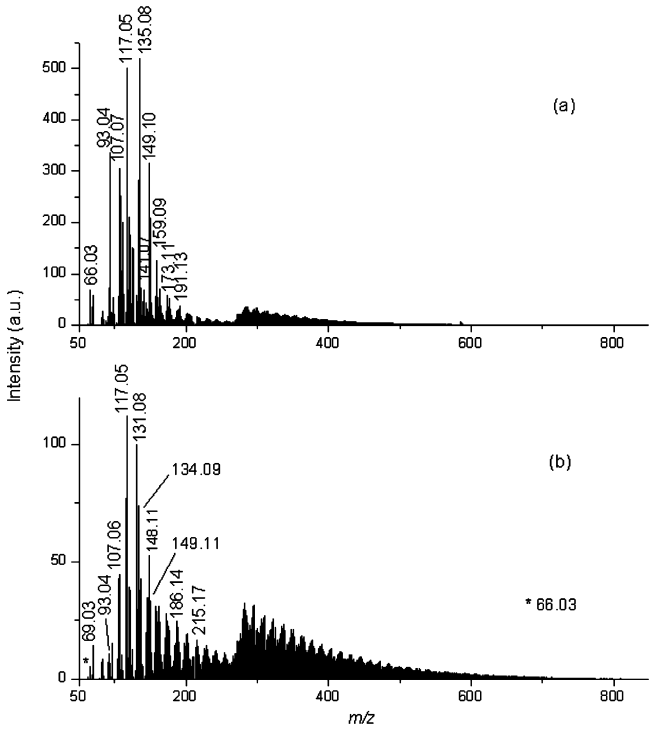

Figure 8. APPI mass spectra of tholins soluble fraction in methanol in negative ion mode: (a) SA98; (b) SA90.

295 and 325 in Figure 6). The resolving power of the time-of-flight analyzer is here insufficient to attribute unambiguously a peak to a single compound, since numerous species of same nominal mass can coexist inside each of the peaks.[16]

Similar clusters could be detected in the toluene soluble fraction (Figure 7), though at very low signal intensity. This not only confirms some very limited solubility of tholins in nonpolar solvents but also confirms a similar pattern in the extracted material in toluene and in methanol.

4.3. Negative Ionization Mode. Complementary results for methanol-extracted samples were obtained under APPI conditions in negative ionization mode. The versatility of the ion formation mechanisms upon APPI has shown to be particularly useful for the analysis of complex mixtures[30] and especially for the determination of nitrogen speciation.[31]

For both SA90 and SA98 soluble fractions, the mass spectra show a large distribution of ions from $m/z = 50$ to m/z 800, organized in regular clusters separated by 13 or 14 u (Figure 8) with a signal at each mass unit, as in positive ion mode. The irregularity in the continuum distribution observed around m/z 260 is due to an instrumental effect from the quadrupole transmission. Superimposed on this continuum, specific ions are observed at m/z 66, 93, 117, and 141 for SA98 (Figure 8a) and m/z 66, 117, 134, and 149 for SA90 (Figure 8b).

Such a peak distribution as observed in Figure 8 is indicative of a polymeric structure. Collision induced dissociation (CID) tandem mass spectrometry experiments have been carried out on some selected ions from the continuum (m/z 283, 284, 285, 297, 310) and on the low mass ions (m/z 66, 93, 117, 134, 141, and 149; see Table 4). The m/z 283, 284, and 285 set was chosen randomly and the fragmentation patterns of these species will

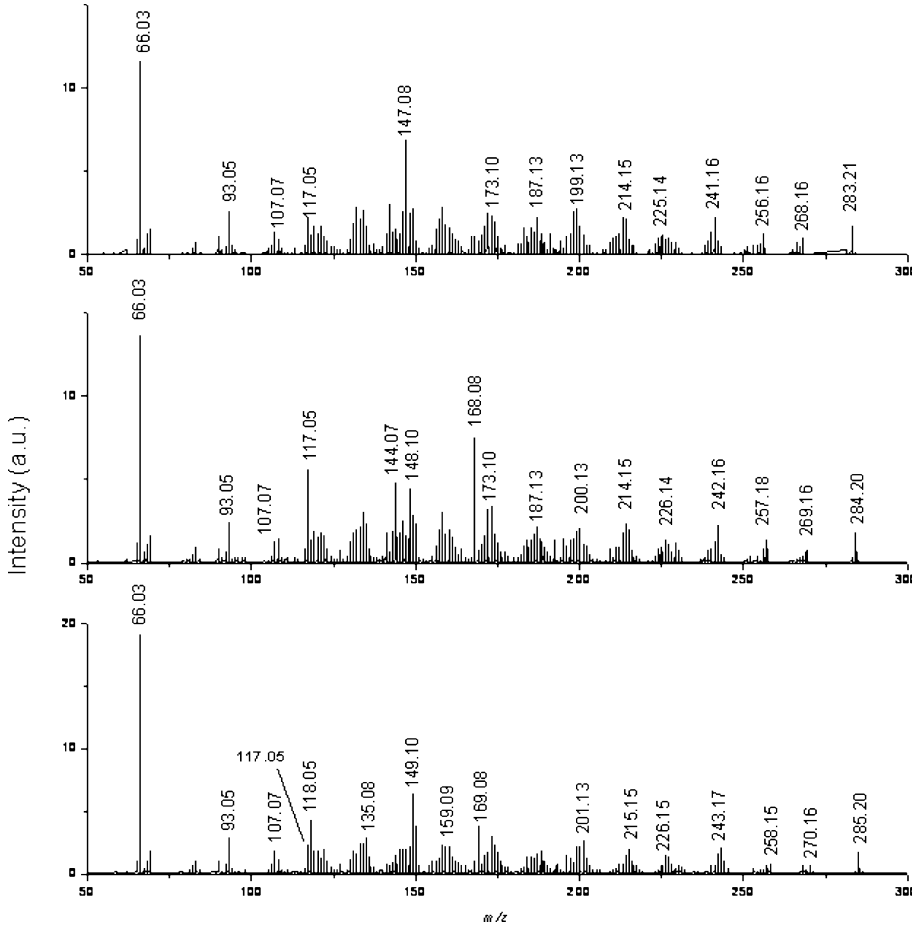

Figure 9. CID mass spectra for the peaks at m/z 283, 284, and 285 of SA98 in the negative ion mode.

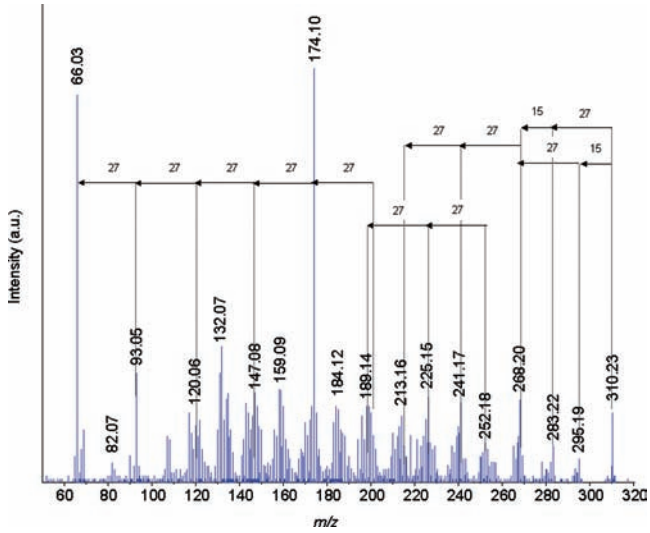

Figure 10. CID mass spectrum for the peak at *m*/*z* 310 of SA98 in the negative ion mode.

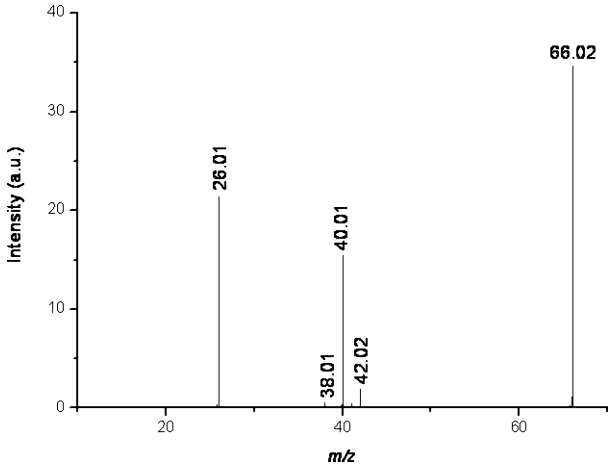

Figure 11. CID mass spectrum for the peak at *m*/*z* 66 of SA98 in the negative ion mode.

be analyzed by comparison. In the same trend of mind, CID of the *m*/*z* 310 ion will be analyzed with respect to the *m*/*z* 283 ion.

Figure 9 compares the MS/MS spectra obtained from the *m*/*z* 283, 284, 285 peaks.

These tandem mass spectra are overall very similar. The initial losses of 15, 17 and 27 u fragments, assigned respectively to neutral CH_3, NH_3, and HCN loss, appear as common features in all the spectra. This clearly indicates that the polymer chains are ended by a methyl, amine, or nitrile groups. It is noteworthy that these chemical functions have been identified by IR spectroscopy (see above). The spectra also show clusters of peaks separated by 13 or 14 u, similarly to full MS observations. Interestingly, several series of peaks connected together by 27 units may be found in the spectra. For example, in the CID spectra of the *m*/*z* 283 and 174 species we can find the following sequences:

$$283 \xrightarrow{-15} 268 \xrightarrow{-27} 241 \xrightarrow{-27} 214 \xrightarrow{-27} 187$$

$$174 \xrightarrow{-27} 147 \xrightarrow{-27} 120 \xrightarrow{-27} 93 \xrightarrow{-27} 66$$

In addition it is very likely that these series are enriched and complexified by intermittent incorporation of 15 u (CH_3) or 17 u (NH_3). Therefore, it seems that the soluble fraction of tholins is mostly made of associated nitrile moiety. To check this hypothesis, the *m*/*z* 310 ion has been analyzed by CID (see Figure 10). The higher mass fragments arise from a loss of 15 u from the precursor and from loss of 27 u to give the *m*/*z* 283 ion, which in turn may lose 15 to produce the *m*/*z* 268 species. Several series of 27 u losses may be identified in this spectrum, the most interesting one being the one connecting the *m*/*z* = 201 peak to the *m*/*z* 66 one through the base peak at *m*/*z* 174.

Finally, the most striking common feature of all the tandem mass spectra is the formation of an intense *m*/*z* 66 peak, whatever the precursor ion selected. Interestingly, the *m*/*z* 66, 93, 107, and 147 peaks are also observed in the full mass spectrum (see Figure 8). These species are found both in the mass spectra and in the CID spectra of all the selected compounds. This could indicate that they are sort of elementary blocks from which the polymerization might occur. Therefore, elucidation of the chemical structure of the *m*/*z* 66 ion, which seems to be the most fundamental of all these ions, appears especially important. The CID spectrum of the *m*/*z* 66 ion is displayed in Figure 11.

At the resolution of the instrument, this signal could correspond to the following formulas: $C_4H_4N^-$, $C_3H_2N_2^-$, $C_5H_6^-$ or $C_2N_3^-$. The $C_5H_6^-$ candidate may be ruled out considering the absence of nitrogen in the formula and the necessary presence of at least one unsaturation involving two carbon centers, which has been excluded by IR spectroscopy. The $C_4H_4N^-$ and $C_3H_2N_2^-$ formulas correspond to either five-member heterocyclic rings (such as pyrrole) or alkyl nitrile derivatives (such as allyl cyanide). Tandem mass spectra of the pure chemicals (pyrrole and allyl cyanide) have been recorded (in the same experimental conditions) to compare with the

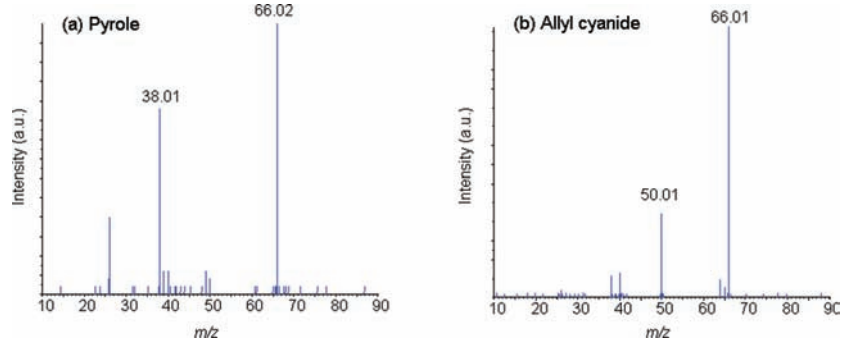

Figure 12. CID mass spectra for the $[M - H]^-$ precursors ions from pyrrole and allyl cyanide standards.

fragmentation pattern of the *m*/*z* 66 ion. As seen in Figure 12, the CID spectra of pyrrole and allyl cyanide are very different from that of the *m*/*z* 66 ion from tholins. The latter shows two main (and complementary) peaks at *m*/*z* 26 and 40, which are assigned to CN^- and CN_2^-, respectively. Therefore, the $C_2N_3^-$ formula appears to us as a good candidate. We propose the following tentative structure and suggest fragmentations as observed upon CID:

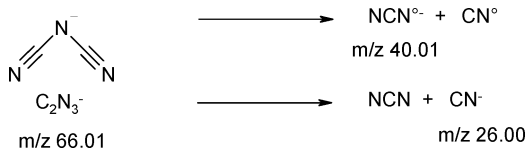

5. Conclusion

The complementary analyses performed in this work lead to a better understanding of the chemical structure of the tholins produced in the PAMPRE reactor. Both SA90 and SA98 samples are significantly soluble in the polar solvent methanol and almost nonsoluble in the nonpolar solvent toluene. Up to 35% of the organic matter was dissolved in the case of SA90 in methanol, which indicates the presence of a major insoluble fraction that constitutes the structural armature of the macroscopic material. Hence, a scanning electron microscope comparison of the samples was conducted and confirmed that almost no variation of the tholins structure took place, regardless of the removal of 35% of material as a soluble fraction in methanol. The IR transmission spectra revealed as well very similar chemical signatures for the soluble and the insoluble fractions (except an evolution of the ratio between aliphatic chains and nitrogen bearing unsaturated functions, such as cyanides). The soluble fractions in methanol and in toluene were finally scrutinized by mass spectral analysis. It highlighted complex but very organized and regular mass spectra, which are very similar in the toluene and methanol solutions, albeit very reduced in the toluene one. This final information is particularly important, as it validates the representative character of methanol extracts as probably containing the fraction of tholins that is sufficiently lightweight to be extracted, but not chemically different from the raw material. This will allow us in future to pursue our efforts in analyzing the soluble fraction. The study by mass spectrometry was pursued with the identification of a common fragmentation pattern by tandem collision induced dissociation analysis in the negative ion mode. A ubiquitous ionic fragment was found at *m*/*z* 66, attributed to the $C_2N_3^-$ pattern. The latter ion being also present as a major ion in the direct negative mass spectrum, it could possibly be an important building brick for the polymerization growth of the tholins. However the resolution of the mass spectrometer used for this study did not allow us to identify the thousands of compounds detected in the soluble fraction of the tholins. Further analysis, requesting for high resolution mass spectrometry are thus in preparation to solve this challenging question.

Acknowledgment. We acknowledge the French program for Planetology (PNP), the PRES UniverSud, the PID OPV, and the French space agency (CNES) for their financial support. We are grateful to Stephan Borensztajn (UPMC Univ Paris 06, UPR 15) for the SEM FEG images.

References and Notes

(1) Coustenis, A.; Achterberg, R. K.; Conrath, B. J.; Jennings, D. E.; Marten, A.; Gautier, D.; Nixon, C. A.; Flasar, F. M.; Teanby, N. A.; Bézard, B.; Samuelson, R. E.; Carlson, R. C.; Lellouch, E.; Bjoraker, G. L.; Romani, P. N.; Taylor, F. W.; Irwin, P. G. J.; Fouchet, T.; Hubert, A.; Orton, G. S.; Kunde, V. G.; Vinatier, S.; Mondellini, J.; Abbas, M. M.; Courtin, R. *Icarus* **2007**, *189*, 35.

(2) Cui, J.; Yelle, R. V.; Vuitton, V.; Waite, J. H., Jr.; Kasprzak, W. T.; Gell, D. A.; Niemann, H. B.; Müller-Wodarg, I. C. F.; Borggren, N.; Fletcher, G. G.; Patrick, E. L.; Raaen, E.; Magee, B. A. *Icarus* **2009**, *200*, 581.

(3) McKay, C. P.; Pollack, J. B.; Courtin, R. *Icarus* **1989**, *80*, 23.

(4) McKay, C. P.; Pollack, J. B.; Courtin, R. *Science* **1991**, *253*, 1 I I8.

(5) Israel, G.; Szopa, C.; Raulin, F.; Cabane, M.; Niemann, H. B.; Atreya, S. K.; Bauer, S. J.; Brun, J.-F.; Chassefière, E.; Coll, P.; Condé, E.; CosciaD. Hauchecorne, A.; Millian, P.; Nguyen, M.-J.; Owen, T.; Riedler, W.; Samuelson, R. E.; Siguier, J.-M.; Steller, M. R. S.; Vidal-Madjar C. *Nature* **2005**, *438*.

(6) Bernard, J.-M.; Coll, P.; Coustenis, A.; Raulin, F. *Planet. Space Sci.* **2003**, *51*, 1003.

(7) Cernogora, G.; Boufendi, L.; Coll, P. *Int. Symp. Plasma Chem. Proc.* **2001**, *4*, 2717.

(8) Coll, P.; Coscia, D.; Smith, N.; Gazeau, M. C.; Ramirez, S. I.; Cernogora, G.; Israel, G.; Raulin, F. *Planet. Space Sci.* **1999**, *47*, 1331.

(9) Imanaka, H.; Khare, B. N.; Elsila, J. E.; Bakes, E. L. O.; McKay, C. P.; Cruikshank, D. P.; Sugita, S.; Matsui, T.; Zare, R. N. *Icarus* **2004**, *168*, 344.

(10) Navarro-González, R.; Ramírez, S. I.; de la Rosa, J. P.; Coll, P.; Raulin, F. *Adv. Space Res.* **2001**, *27*, 271.

(11) Sagan, C.; Khare, B. N. *Nature* **1979**, *277*, 102.

(12) Sagan, C.; Thompson, W. R. *Icarus* **1984**, *59*, 133.

(13) Vanssay, E.; Gazeau, M.-C.; Guillemin, J. C.; Raulin, F. *Planet. Space Sci.* **1995**, *43*, 25.

(14) Szopa, C.; Cernogora, G.; Boufendi, L.; Correia, J.-J.; Coll, P. *Planet. Space Sci.* **2006**, *54*, 394.

(15) McKay, C. P. *Planet. Space Sci.* **1996**, *44*, 741.

(16) Sarker, N.; Somogyi, A.; Lunine, J. I.; Smith, M. A. *Astrobiology* **2003**, *3*, 719.

(17) Niemann, H. B.; Atreya, S. K.; Bauer, S. J.; Carignan, G. R.; Demick, J. E.; Frost, R. L.; Gautier, D.; Haberman, J. A.; Harpold, D. N.; Hunten, D. M.; Israel, G.; Lunine, J. I.; Kasprzak, W. T.; Owen, T. C.; Paulkovich, M.; Raulin, F.; Raaen, E.; Way, S. H. *Nature* **2005**, *438*, 779.

(18) Hadamcik, E.; Renard, J.-B.; Alcouffe, G.; Cernogora, G.; Levasseur-Regourd, A.-C.; Szopa, C. *Planet. Space Sci.* 2009. in press.

(19) Somogyi, A.; Oh, C.-H.; Smith, M. A.; Lunine, J. I. *Am. Soc. Mass Spectrom.* **2005**, *16*, 850.

(20) Flory, P. J. *J. Chem. Phys.* **1941**, *9*, 660.

(21) Flory, P. J. *J. Chem. Phys.* **1942**, *10*, 51.

(22) Huggins, M. L. *J. Chem. Phys.* **1941**, *9*, 440.

(23) Huggins, M. L. *J. Am. Chem. Soc.* **1942**, *64*, 1712.

(24) Raulin, F. *Adv. Space Res.* **1987**, *7*, 71.

(25) Quirico, E.; Montagnac, G.; Lees, V.; McMillan, P. F.; Szopa, C.; Cernogora, G.; Rouzaud, J.-N.; Simon, P.; Bernard, J.-M.; Coll, P.; Fray, N.; Minard, R. D.; Raulin, F.; Reynard, B.; Schmitt, B. *Icarus* **2008**, *198*, 218.

(26) Derenne, S.; Quirico, E.; Szopa, C.; Cernogora, G.; Schmidt, B.; Less, V.; McMillan, P. F. 39th Lunar and Planetary Science Conference, (Lunar and Planetary Science XXXIX), held March 10−14, 2008 in League City, Texas. LPI -Contribution No. 13912008.

(27) Rodil, S. E.; Ferrari, A. C.; Robertson, J.; Milne, W. I. *J. Appl. Phys.* **2001**, *89*, 5425.

(28) Robb, D.; Blades, M. W. *Anal. Chim. Acta* **2008**, *627*, 34.

(29) Robb, D. B.; Covey, T. R.; Bruins, A. P. *Anal. Chem.* **2000**, *72*, 3653.

(30) Mopper, K.; Stubbins, A.; Ritchie, J. D.; Bialk, H. M.; Hatcher, P. G. *Chem. Rev.* **2007**, *107*, 419.

(31) Purcell, J. M.; Rodgers, R. P.; Hendrickson, C. L.; Marshall, A. G. *J. Am. Soc. Mass Spectrom.* **2007**, *18*, 1265.

JP904735Q